Error Function–Based Evaluation of Linear and Non-Linear Isotherms for Rhodamine B Adsorption on Green-Synthesized CaO Nanoparticles

Gulnaz Nasir[1], Fozia Batool[1*], Tunzeel Iqbal[2], Noreen Sajjad[3], Shoomaila Latif[4], Maryam Siddiqa[1], Eman Shehzad[1], Misbah Tahira[1], Muhammad Mustaqeem[1], Allah Ditta[5,6*], Graciela Dolores Avila-Quezada[7], Mohamed A. Mattar[8*]

[1]Institute of Chemistry, University of Sargodha, Sargodha 40100, Pakistan

[2]Department of Chemistry, The Rawalpindi Women's University, Rawalpindi, Pakistan

[3]Department of Chemistry, University of Lahore, Lahore 54590, Pakistan

[4]School of Physical Sciences, University of Punjab, Lahore 54590, Pakistan

[5]Department of Environmental Sciences, Shaheed Benazir Bhutto University Sheringal, Dir (U), Khyber Pakhtunkhwa 18000, Pakistan

[6]School of Biological Sciences, The University of Western Australia, 35 Stirling Highway, Perth, WA 6009, Australia

[7]Facultad de Ciencias Agrotecnológicas, Universidad Autónoma de Chihuahua, 31350, Chihuahua, Chihuahua, México

[8] Department of Agricultural Engineering, College of Food and Agriculture Sciences, King Saud University, Riyadh 11451, Saudi Arabia

*Correspondence: fozia.batool@uos.edu.pk (FB), allah.ditta@sbbu.edu.pk (AD), mmattar@ksu.edu.sa (M.A.M.)

ABSTRACT

Adsorption is recognized as one of the most impactful techniques extensively utilized in worldwide environmental protection activities. Interpreting experimental adsorption isotherm data is essential for predicting the mechanism of adsorption. This study involves the comparison and discussion of linear and non-linear forms of Langmuir, Freundlich, Dubinin-Radushkevich, and Temkin isotherms, which were applied to the experimental data obtained during the adsorption of Rhodamine-B dye by CaO NPs. To determine the best-fitting model in the adsorption isotherms, and to quantitatively illustrate the relevant sorption system, different error functions, and statistical tools including the sum of squares of the errors (ERRSQ/RSS), average relative error (ARE), the sum of absolute errors (EABS), average percentage error (APE/ARED), second-order corrected Akaike information criterion (ALC_c), chi-square test (Chi-Sq/χ^2), G^2, Hybrid fractional error function (HYBRID), a standard procedure called the sum of normalized errors (SNE), and fit tools including the coefficient of determination (R^2), student's T-test, and F-tests were applied. The results indicated that the Langmuir isotherm was identified as more suitable (T-test = 0.999981, F-test = 0.991724664, and R^2 = 0.98537) than all other linear forms. Likewise, the analysis of non-linear forms provided the Temkin model as more beneficial, with the lowest values of all error functions and the largest values of fit tools, including R^2 (0.94687), T-test (0.969513), and F-test (0.999998). The linear Langmuir model was noted as best fitted with the largest values of fit tools and lowest normalized errors (0.0077098) than the non-linear Langmuir isotherm (0.306951). It was concluded that the linear Langmuir adsorption isotherm has the lowest values of all error functions, including SNE, and the highest values of fit tools among linear forms of each adsorption model. Moreover, the non-linear Temkin isotherm was determined as the best-fitting model among

all non-linear forms, with the minimum values of all error functions, and maximum values of good fit tools.

Keywords: Adsorption isotherms; Comparison; Error analysis; Linear and non-linear methods; Rhodamine-B.

1. INTRODUCTION

The industrial sector involves the wide application of adsorption processes, including cleaning process streams and removing pollutants from wastewater (Sayed et al., 2024a,b; Chauhan et al., 2025; Nisar et al., 2025). Even though adsorption is widely used in industrial settings, these processes entail a complex web of physicochemical phenomena, including intraparticle diffusion, the kinetics of adsorption at the adsorbent site, and the mass transfer of chemical species from the fluid phase to adsorbent particles (Hanafiah et al., 2024; Selvanarayanan et al., 2024). Although the process of adsorption is very complex, the first and most important step in this study is the determination of the adsorption isotherm and the parameters of that model. The isothermal equations show the link between the fluid and solid phases' concentrations and characterize the adsorption process's equilibrium conditions at a specific temperature. Thus, a precise mathematical representation of an equilibrium isotherm is crucial for the efficient design of sorption systems.

Many isotherm models can be used to analyze experimental data and understand how adsorption takes place. It is not possible to use a specific method for selecting the best-fit isotherm. Currently, non-linear or linear equations are applied to determine the isotherm constants with one adsorbate (Liu et al., 2024; Mahesh et al., 2024). Nowadays, the non-linear regression method is believed to be the most efficient way to find the optimal isotherm. Optimal adsorption isotherms are calculated using the least squares technique, as reported by several researchers (Kumar and Porkodi, 2006;

Abdulhameed et al., 2025). An error function is needed to apply this method. When the differences between the data used for calculations and the observed results are small, the isotherm parameters can be determined. It has also been noticed that sometimes the parameters obtained from linear regression differ from those gained through non-linear regression (Slimani et al., 2014). The non-linear technique works towards minimizing the variation between the experimental results and what is expected from the isotherm.

During recent years, researchers have relied on methods such as the coefficient of determination, sum of squared errors, hybrid error functions, average relative error, and the sum of absolute errors to find the optimal isotherm equation (Paluri et al., 2022; Umeh et al., 2024; Venkatraman et al., 2024; Radha et al., 2025; Suresh et al., 2025). The focus is on linear regression alongside isotherm models named Langmuir, Freundlich, Dubinin-Radushkevich, and Temkin. These isotherms are chosen in this study due to their wide range of assumptions and their applicability, which gives extensive insights into the adsorption process and the interactions between the adsorbate and adsorbent. Non-linear regression analysis was applied to these adsorption isotherms, and a comparison was made between linear and non-linear regression techniques. Furthermore, the results were examined for their accuracy and overall fit using the errors and statistical methods previously mentioned. This work involves the application of linear and non-linear adsorption isotherms for the adsorption of Rhodamine-B dye on CaO nanoparticles. Moreover, the environmentally friendly synthesis of CaO nanoparticles through the utilization of a novel green material of Mulberry leaf extract. Instead of chemical-based reducing agents, the green extract is employed to synthesize CaO NPs with excellent properties for the remediation of Rhodamine B from wastewater. The primary objective of this study was to assess the suitability of statistical methods in determining the outfitting isotherm model. Thus, for both linear and non-linear forms

of adsorption, various error functions were applied to facilitate the decision for the best-fit data set. To our knowledge, no study has been conducted on normalizing and combining the error results, a procedure called the sum of normalized errors for each set of parameters from which the lowest normalized error set was selected.

2. MATERIALS AND METHODS

The method involved the green synthesis of calcium oxide nanoparticles by employing the Mulberry leaf extract. These nanoparticles were applied for the adsorption of Rhodamine B dye. All chemicals were obtained from Sigma Aldrich with 98% purity, and Mulberry leaves were collected from the Botanical Garden of the University of Sargodha. After the extraction of the leaf extract, it was employed for the green synthesis of Cao NPs. For the synthesis purpose, 1.64 g of Calcium nitrate was dissolved in 100 mL of water to prepare a solution. A 10 mL leaf extract was mixed with 10 mL of calcium nitrate solution and heated with constant stirring. Sodium hydroxide was added dropwise to the above solution which resulting in the formation of white precipitates of CaO NPs. Synthesized NPs were filtered, dried, and used for adsorption purposes (Figure 1). Various characterization techniques characterized the bio-synthesized adsorbent. The dye stock solution was prepared by dissolving 1g of Rhodamine-B into 1000 mL of distilled water. This solution was further diluted for various adsorption experiments.

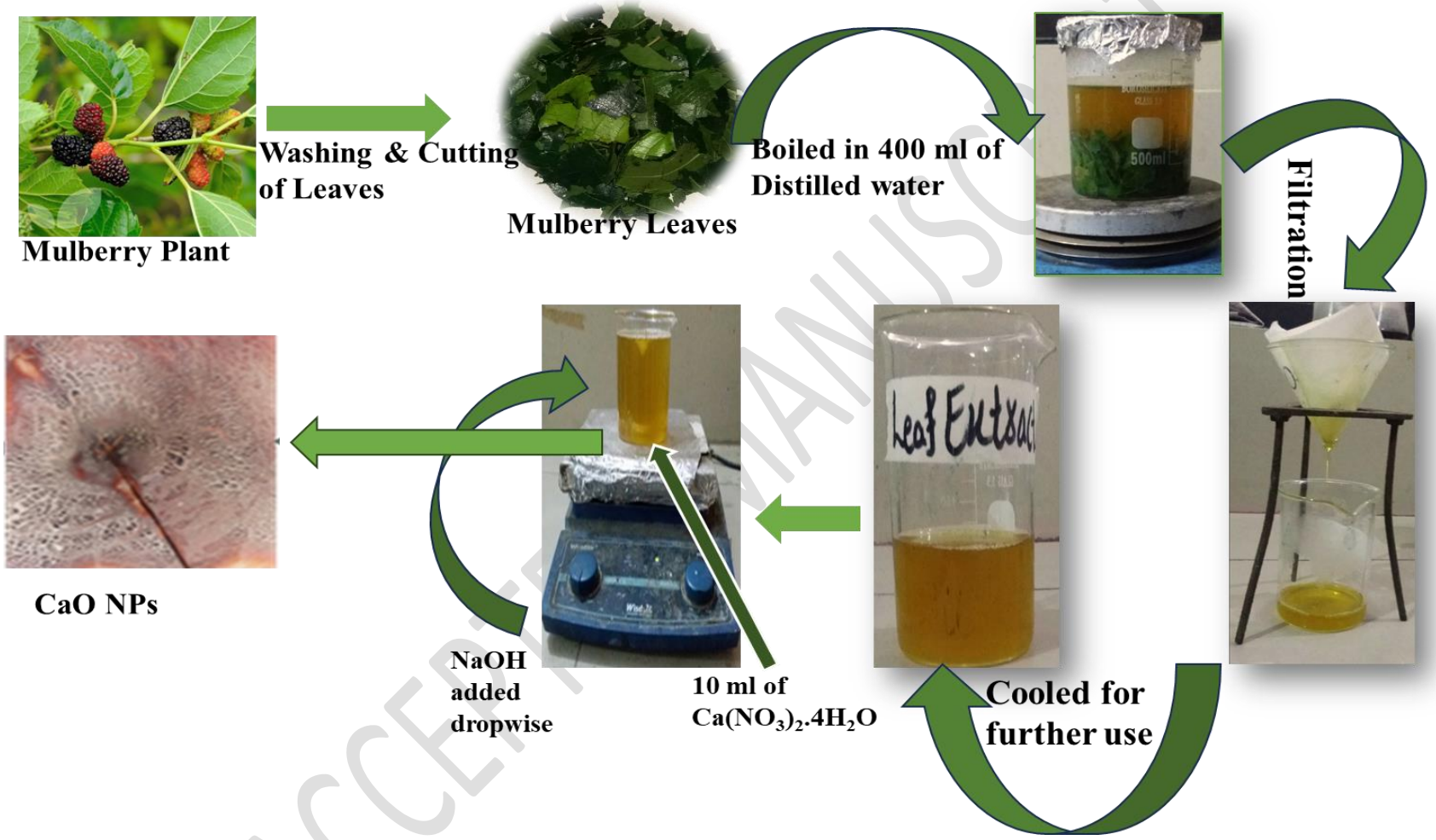

Figure 1. Scheme of Synthesis of CaO NPs

2.1. Investigations and experimental procedures

The effect of various experimental parameters including the initial concentration dye (varied from 20 to 100 ppm), amount of adsorbent (0.2 to 0.6 g), pH (2 to 10), temperature (30 to 70 °C), and effect of contact time (30 to 150 minutes) on the adsorptive removal of Rhodamine-B dye by CaO NPs was studied in batch mode. In every adsorption experimental procedure, the solution of the dye with the adsorbent was shaken using the orbital shaker at a constant speed of 150 rpm. Rhodamine-B dye's residual concentration was measured using a UV-visible spectrophotometer at 550 nm wavelength absorption for Rhodamine-B dye. Various adsorption isotherms, kinetics, and thermodynamics were applied to the experimental data. Linear and non-linear forms of adsorption isotherms are studied, and their analysis by error functions to determine the best-fitted model is provided below.

2.2. Linear forms of isotherm models

Because they are easy to calculate, linear interpretations of adsorption isotherms are typically employed to choose the most appropriate model for the adsorption system or to calculate the isotherm parameters. In this study, linear forms of four types of adsorption isotherms, including Langmuir, Freundlich, Dubinin-Radushkevich, and Temkin, are used to determine the best-fitting model for the adsorption of Rhodamine-b dye by CaO NPs. It describes the process of adsorption onto a surface with a known number of sites by forming just one monolayer (Chen et al., 2025). On the X-axis, this graph includes $1/C_e$, and on the Y-axis, it has $1/q_e$. In this example, q_e shows the amount adsorbed at equilibrium by a certain weight of material, and C_e refers to the concentration of the adsorbate (mg L^{-1}) at equilibrium. The values for q_{max} and K_L for the Langmuir isotherm are found by analyzing the slope and intercept of the line on the graph.

Unlike the Langmuir approach, the Freundlich model examines the adsorption of molecules in more than one layer (Freundlich, 1906). The values of K_F and n_F in the Freundlich model come from the slope and intercept in the graph. For this case, the dimensionless adsorption intensity is n_F, and the Freundlich isotherm constant is K_F (mg g^{-1} (mg L^{-1}) $^{-1}$/n).

Nasir et al. (2025) suggest that the Dubinin-Radushkevich isotherm is used to study how adsorption happens on a heterogeneous surface. The isotherm is employed to explore the distinction between physical and chemical adsorption (Dubinin, 1960). When drawing this model's graph, ε^2 is plotted against lnqe. K_{DR} is the constant (mol^2 kJ^{-2}) used in the Dubinin-Radushkevich model, ε is the Polanyi potential (mol^2 kJ^{-2}), and q_{mDR} stands for the maximum possible capacity on the isotherm (mg g^{-1}).

The Temkin model explains various ways that the adsorbate and the adsorbent can influence one another. It implies that the heat of adsorption gets lower when the area of coverage is larger (Temkin, 1940; Nasir et al., 2025). Slope and intercept are used to work out the K_T and B_T of a line.

2.3. Non-linear forms of adsorption isotherms

Some computer-related techniques have been developed to try out different parameters, to investigate the characteristics of non-linear isotherms. In addition, the scientists study non-linear adaptations of the Langmuir, Freundlich, Dubinin-Radushkevich, and Temkin isotherms. The parameters are determined and checked against the linear equations, so the appropriate and most suitable model can be found for absorbing Rhodamine-B dye. The graph showing the Langmuir isotherm uses the values of C_e versus q_e.

The Freundlich model is the first to illustrate reversible adsorption processes that occur at non-ideal conditions. In the case of the non-linear representation, the graph is plotted with C_e against qe, and K_F and n_F are derived from the graph.

Another empirical model, initially developed to illustrate the adsorption process using a pore-filling mechanism, is the Dubinin-Radushkevich model. The graph of C_e vs q_e is plotted for the non-linear form of this isotherm to obtain the parameters such as the maximum monolayer adsorption capacity predicted by the Dubinin–Radushkevich isotherm (q_{mDR}) and the Dubinin–Radushkevich constant (K_{DR}). Similarly, the non-linear form of the Temkin isotherm is plotted with C_e vs q_e isothermal parameters, including K_T and B_T determined from this graph.

3.3. Error functions and statistical tools

An analytical model that shows a dataset is called a best-fit model. This model is utilized to identify the parameters that correctly describe and identify the dataset, as well as the adsorption process and isotherms. The error function indicates the differences between the dataset and the best-fit model. Statistical functions are used to determine the suitability of the fit, the similarity among the different groups, and the correlation (Mahajan et al., 2023). For both linear and non-linear forms of adsorption isotherms, the following error functions which are applied include chi-square test (Chi-Sq/χ^2), hybrid fractional error function (HYBRID), coefficient of determination (R^2), the sum of normalized errors (SNE), average relative error (ARE), the sum of absolute errors (EABS), average percentage error (APE/ARED), second-order corrected Akaike information criterion (ALCc), student's T-test, and F-test. These functions are utilized to compare the best applicability of linear and non-linear regression methods and to find the most accurate isotherm model for the experimental equilibrium data. The smaller the values of all error functions, and the larger the values of R^2, T-test, and F-test, the more accurate the isotherm model.

3.3.1. The sum of squares errors (RSS/ERRSQ)

It is among the frequently used error functions (Kumar and Sivanesan, 2006). Higher liquid-phase concentration levels tend to increase the intensity of error values and, consequently, squared errors. This results in a more precise fit for the determination of isotherm parameters.

3.3.2. Average relative error deviation (ARED/APE%)

Marquardt introduced the ARED to minimize the fractional error distribution throughout the full range of concentrations. This model distorts the experimental data (Kapoor and Yang, 1989).

3.3.3. The sum of absolute errors (EABS)

This function is like the ERRSQ, as the error increases, a better fit will be suggested, emphasizing the data with higher concentrations (Voudrias et al., 2002).

3.3.4. Hybrid error function (HYBRID)

Created by Kapoor and Yang (1989), it optimizes the fit of ERRSQ at a decreased concentration by normalizing with the measured value.

3.3.5. Coefficient of determination (R^2)

R^2 falls within the range of 0 to 1 due to its squared form, ensuring positivity (Kumar and Sivanesan, 2006).

3.3.6. Chi-Sq/$\chi 2$

Employing this non-linear analysis is crucial to ensure the optimal fit of an adsorption system. A better one will have the lowest values of χ^2, which diminishes the deviation between the experimental and theoretical values (Rana and Singhal, 2015).

3.3.7. G^2 test-statistic

The natural logarithm of the ratio obtained by dividing the observed number by the projected number is the G^2 test statistic. Each logarithm is multiplied by the observed number, and the results

are then put together and doubled. It is alternatively known as the log-likelihood test or likelihood ratio test (Aslam et al., 2024).

3.3.8. Sum of normalized errors (SNE)

Using several error functions has the drawback of producing too many parameters for the isotherms to compare. The researchers use a conventional approach known as the sum of the normalized error to predict a meaningful comparison among the sets of parameters and to determine the best-fitting isotherm (Kapoor and Yang, 1989; Akhtar et al., 2024). The parameter set that results in the smallest values of the sum of normalized error is regarded as optimal for the provided isotherm.

3.3.9. Students' T-test

The purpose of this test is to ascertain whether the two datasets differ significantly from one another. Specifically, it contrasted the computed and observed data, which show the modeled and experimental equilibrium solid-state adsorption capabilities, respectively. The paired T-test with a two-tailed distribution was performed for the applied isotherm models utilizing the formula function in Microsoft Excel (Mahajan et al., 2023).

3.3.10. F-test

The F-test is applied to verify the goodness of fit between the observed and experimental data. The function was directly computed using the formula syntax of Microsoft Excel (Outram et al., 2021).

3. RESULTS AND DISCUSSIONS

3.1. Linear fitting of the isotherm models

Linear forms of four adsorption isotherms, including Langmuir, Freundlich, Dubinin-Radushkevich, and Temkin, are represented in Figure 2. The isothermal parameters and their

correlation coefficient are summarized in Table 1. In the Langmuir isotherm, the monolayer adsorption capacity for the formation of the monolayer of Rhodamine-B onto the CaO NPs was 57.5373 mg g^{-1}. The favorability of the Langmuir model for adsorption purposes is analyzed by a dimensionless factor R_L. If R_L ranges from 0 to 1, it indicates the best applicability of the Langmuir isotherm to the adsorption system. Table 1 shows that the value of R_L calculated for this isotherm is in this range. Moreover, the value of R^2 for the Langmuir model is close to unity, which shows that this model is compatible with the present work.

In the Freundlich isotherm, the adsorption intensity ($1/n_F$) ranges from 0 to 1, which reflects the favorable adsorption (Lavecchia et al., 2024). In addition, adsorption is known to be either physical or chemical, depending on whether nF is greater than or less than one, respectively (Ifelebuegu, 2012). So, the adsorption process was simple to happen when 1/n was less than 1, but it became more difficult when 1/n was greater than 1 (Mohamed et al., 2025). Since nF is greater than 1, the study demonstrates physical adsorption, while 1/nF is 0.86821, which agrees with other studies that showed Rhodamine-B adsorbed favorably (Foo and Hameed, 2010).

Thanks to the Dubinin-Radushkevich isotherm, identifying whether sorption is physical or chemical can be much easier. When E is less than 8 kJ mol^{-1}, the process is called physisorption, and when E is from 8 to 16 kJ mol^{-1}, it is known as chemical adsorption. Here, the E value is higher than 8 kJ mol^{-1}, which proves that chemical adsorption occurs. Based on previous work, the R^2 value reveals that this model is ideal for the current adsorption system (Inyinbor et al., 2016).

By analyzing the Bartlett temperature, we can recognize whether physisorption or chemisorption is taking place on a solid. When BT is less than 1, the adsorption happens due to physisorption (Latif et al., 2025). Since the BT in Table 1 equals 0.62, this suggests that adsorption is a physical process. Also, the R^2 value demonstrates whether the model is appropriate for the study of

adsorption at hand. It has been found that the adsorption of Rhodamine-B by CaO NPs is accomplished by both physicochemical and chemical processes. Several scientific works suggest that the surface can have both physical and chemical adsorption by allowing both types of layers to be present on top of surface molecules (Dixit et al., 2024; Kanwal et al., 2024). The fact that the Langmuir isotherm gets a higher R^2 value than the others proves it is the best-suited model for the adsorption of Rhodamine-B onto CaO NPs.

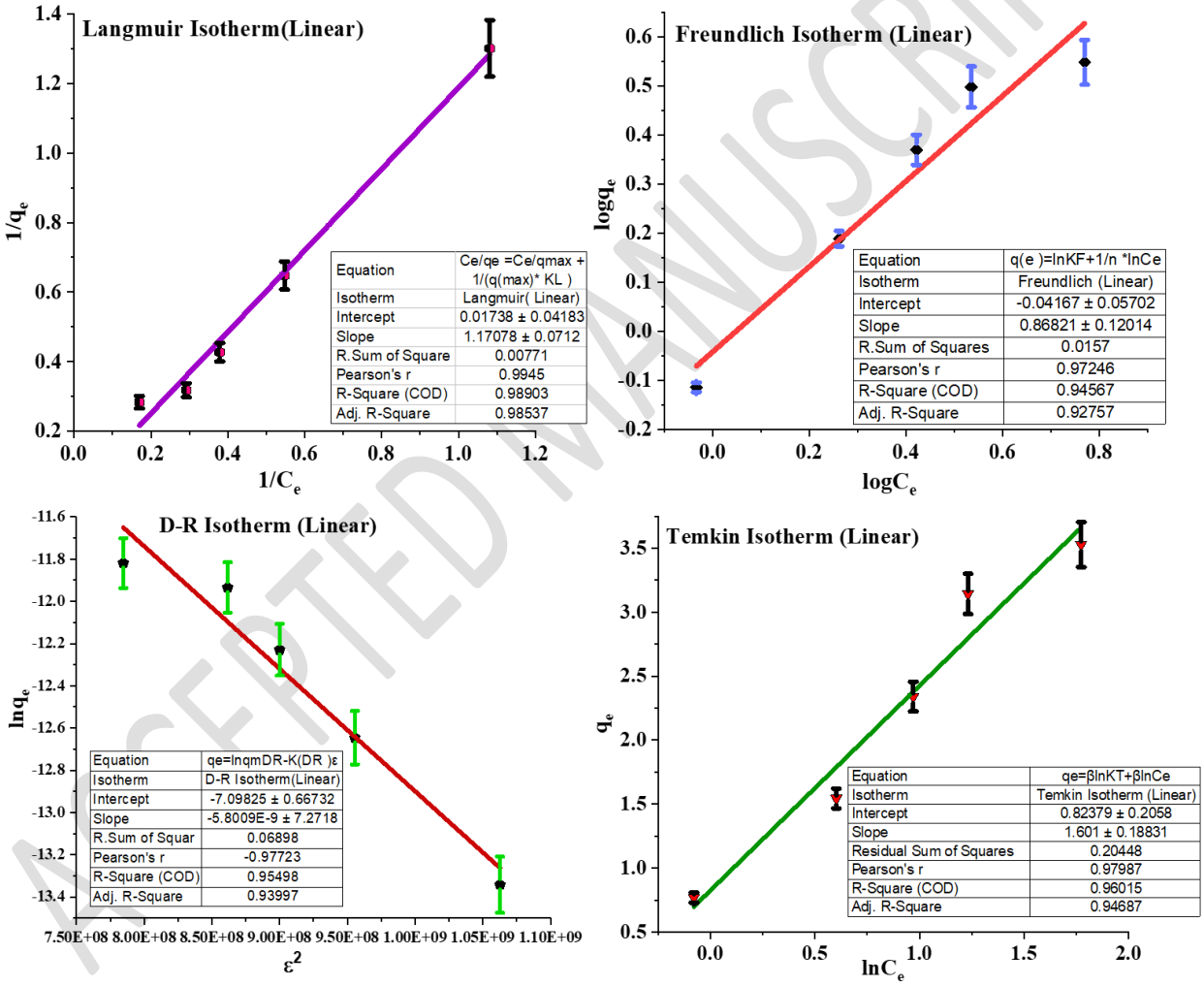

Figure 2. Linearized isotherm models show rhodamine-B adsorption by CaO NPs

Table 1. Linearized isotherm parameters. Where RL = separation factor, q_{max} = the maximum theoretical amount of a substance that an adsorbent can hold per unit mass of the adsorbent, K_L = Langmuir constant, R^2 = coefficient of determination, K_F = Freundlich constant, nF = adsorption intensity, q_{mDR} = the maximum possible capacity on the isotherm (mg g^{-1}), K_{DR} = Dubinin-Radushkevich constant, K_T = Toth isotherm constant, and B_T = Temkin isotherm constant

Isotherms (Linear-Forms)	**Characteristic parameters of corresponding isotherms for adsorbate (rhodamine-B dye) and adsorbent (CaO NPs)**			
Langmuir	R_L= 0.7710718	q_{max} = 57.53739931	K_L=0.014844804	R^2 = 0.98537
Freundlich	K_F = 0.908510603	$1/n_F$ = 0.86821	n_F =1.171795	R^2 = 0.92757
Dubinin-Radushkevich	q_{mDR} = 0.00082655	K_{DR} = 5.80E-09	E=9.28E+03	R^2 = 0.93997
Temkin	K_T = 3.739320087	B_T = 0.624609619	-	R^2 = 0.94687

3.2. Non-linear fitting of isothermal models

Non-linear forms of the four adsorption isotherms are given in Figure 3. The values of their isothermal parameters, including values of correlation coefficients, are given in Table 2. The higher values of R^2 are obtained by the non-linear fitting of Temkin (R^2 = 0.94687), Dubinin-Radushkevich (R^2 = 0.93745), and the Langmuir model (R^2 = 0.92024) as compared to the Freundlich adsorption isotherm. The comparison of R^2 signifies that the Temkin, Dubinin-Radushkevich, and Langmuir isotherms best fit the experimental data, whereas the Freundlich isotherm model cannot. Moreover, the maximum adsorption capacity values obtained using the non-linear form of the Langmuir and Temkin models fit closely with the experimental data. This illustrates these isotherms' ideal and successful modeling of the present adsorption systems. The fitting of non-linear models by comparing R^2 values follows the pattern. Temkin > Dubinin-Radushkevich > Langmuir > Freundlich. However, a valuable and accurate comparison can be

obtained by using the various error functions rather than only R^2 analysis (Benmessaoud et al., 2020).

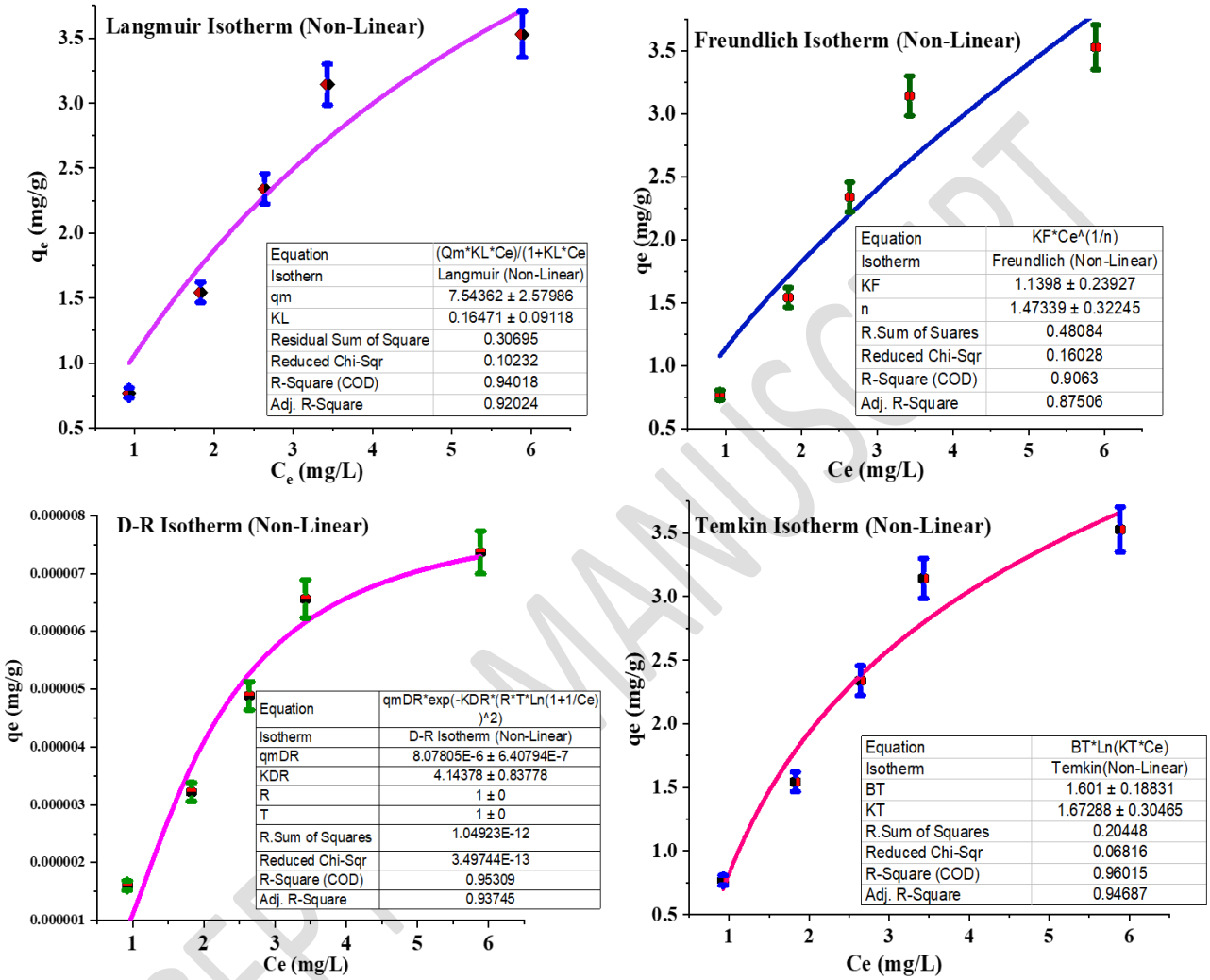

Figure 3. Non-linearized isotherm models showing rhodamine-B adsorption by CaO NPs

Table 2. Non-linearized isotherm parameters where q_{max} = the maximum theoretical amount of a substance that an adsorbent can hold per unit mass of the adsorbent, K_L = Langmuir constant, R^2 = coefficient of determination, K_F = Freundlich constant, q_{mDR} = the maximum possible capacity on the isotherm (mg g^{-1}), K_{DR} = Dubinin-Radushkevich constant, K_T = Toth isotherm constant, and B_T = Temkin isotherm constant

Isotherms (Non-linear forms)	**Characteristic parameters of corresponding isotherms for adsorbate (Rhodamine-B dye) and adsorbent (CaO NPs)**
Langmuir	q_{max} = 7.54362 K_L = 0.1647 R^2 = 0.92024
Freundlich	K_F = 1.1398 1/n = 0.6787 R^2 = 0.87506
Dubinin-Radushkevich	q_{mDR} = 8.07805E-6 K_{DR} = 4.14378 R^2 = 0.93745
Temkin	K_T = 1.67288 B_T = 1.601 R^2 = 0.94687

3.3. Error analysis for optimization of linear isotherms

To identify the availability of linear adsorption isotherms and to determine the best fitting isotherms, various error functions were applied, and their values are depicted in the Table. 3. A comparison was made between linear forms to identify the best applicable model among all linear forms of adsorption isotherms. The Langmuir isotherm value of Chi-Sq/χ^2, G^2, and HYBRID is less than Temkin but higher than the Freundlich and Dubinin-Radushkevich isotherms. The values of ARE and APE (%) are below Freundlich's but higher than the Dubinin-Radushkevich and

Temkin models. The values of RSS and ALC_c are lower than all other isotherms. In the Freundlich isotherm, the values of Chi-Sq/χ^2, EABS, HYBRID, and G^2 are lower than those of Langmuir and Temkin but superior to the Dubinin-Radushkevich isotherm. But its values of ARE and APE are highest among all other isotherms, and the values of RSS and ALC_c are lower than Dubinin-Radushkevich and Temkin, but higher than the Langmuir model. The comparison of error function values of the Dubinin-Radushkevich model indicates that its Chi-Sq/χ^2, EABS, ARE, HYBRID, and G^2 are the lowest among all linear forms of other isotherms. Al_{Cc} is also less than all the isotherms, except the Langmuir model. APE is lower than Langmuir and Freundlich, but higher than the Temkin isotherm. When Temkin's error functions are contrasted with the error functions of all other isotherms, it demonstrates the following results are demonstrated. Its Chi-Sq/χ^2, $G^{2,}$ RSS, and HYBRID function values exceed all other models. APE value is under all other models, EABS value is lower than Langmuir but larger than Dubinin-Radushkevich and Freundlich isotherms, ARE is smaller than Freundlich and Langmuir, but above than Dubinin-Radushkevich model, and ALC_c value dominates all isotherms. The values of these error functions make it difficult to choose the best-aligned model. Thus, a valuable comparison is made using the good fit functions, including the Student's T-test, F-test, R^2, and SNE. Enhanced values of R^2, student's T-test, F-test, and the smallest value of SNE suggest the most accurate model (Hadi et al., 2010). When these error functions of all isotherms were compared, the subsequent outcomes were recorded.

T-Test = **Langmuir** > Temkin > Freundlich > Dubinin-Radushkevich

F-Test = **Langmuir** > Temkin> Dubinin-Radushkevich > Freundlich

R^2 = **Langmuir** > Temkin > Dubinin-Radushkevich > Freundlich

SNE = Freundlich > Temkin > Dubinin-Radushkevich > **Langmuir**

It is evident from the result that the values of the T-test, F-test, and R^2 are dominant for the Langmuir isotherm against all other models, and its value of SNE is the smallest of all other isotherms. As is also clearly indicated in Figure 4. When the fit tools values of each linear form of the adsorption isotherm were drawn graphically. This highlights the Linear form of the Langmuir adsorption isotherm excellent fit model compared to other models for the adsorption of Rhodamine-B dye, as documented in the literature (Batool et al., 2025; Usman et al., 2025). Thus, the order of fitting of linear models is Langmuir > Dubinin-Radushkevich > Temkin > Freundlich.

Table 3. Values of error functions and fit tools of linearized models (Nebaghe, El Boundati et al., 2016)

Error function model	**Isotherm model (Linear)**			
	Langmuir	**Freundlich**	**Dubinin-Radushkevich**	**Temkin**
ERRSQ/RSS	0.0077098	0.015699	0.068980854	0.204481724
EABS	8.65288E-06	-3.2E-06	-3.94894E-05	1.21E-06
ARE	0.139893444	2.594482	-0.002	-0.05725
ARED/APE (%)	0.559573776	10.37792837	-0.008	-0.22899
Chi-Sq/χ^2	0.024175	0.011897	-0.00573	0.08930425
HYBRD	0.604371313	0.29742921	-0.14327	2.232606
ALC_c	-31.573479	-28.0179	-20.61682099	-15.1836
G^2	0.026725748	0.006895	-0.00581171	0.088950597
Students' T-test	**0.999981**	0.999982	0.99989	0.999998
F-test	**0.991724664**	0.958126973	0.965461529	0.969513
SNE	**-29.54254804**	-1.326648338	-20.68916502	-5.32761018
R^2	**0.98537**	0.92757	0.93997	0.94687

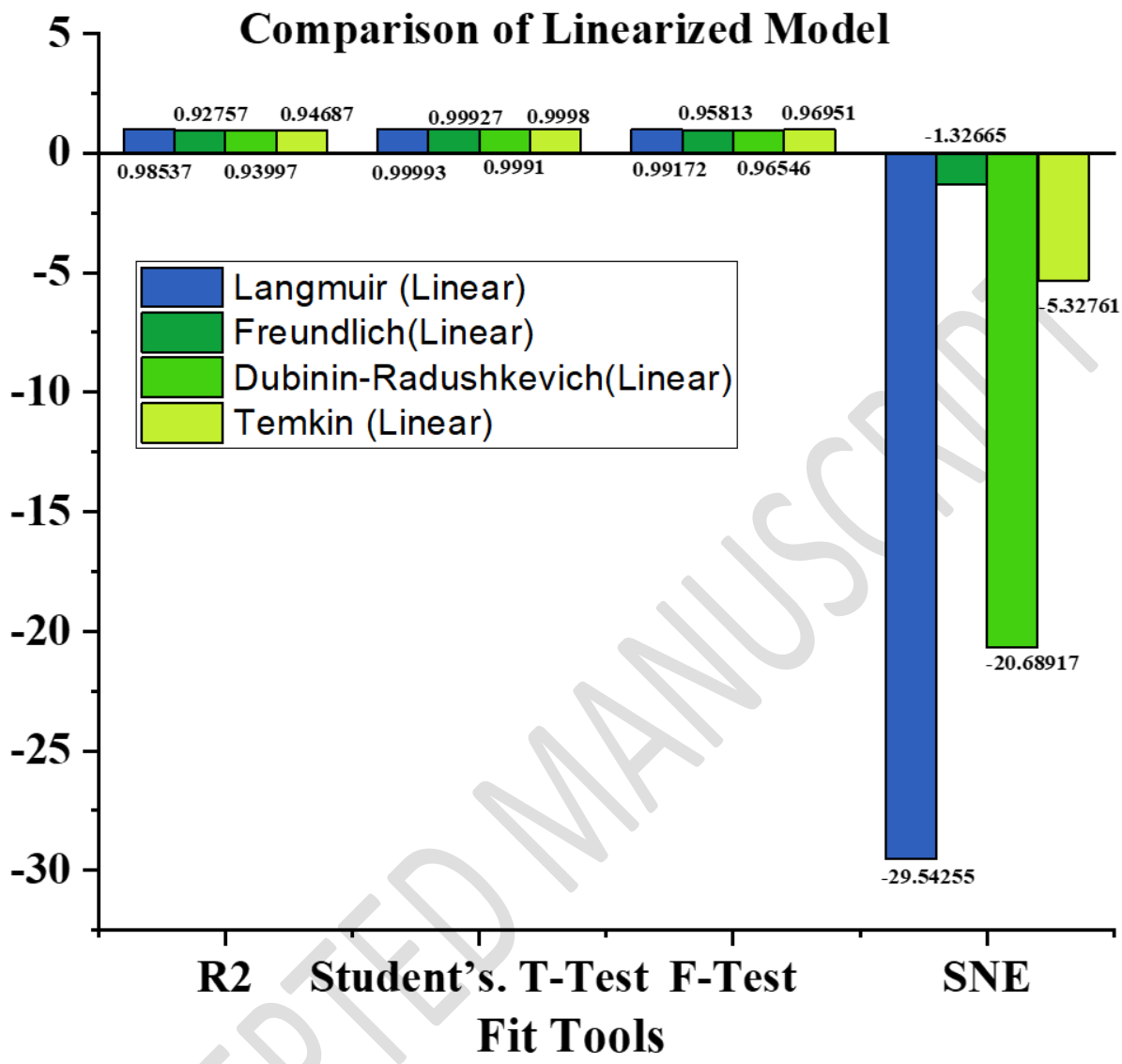

Figure 4. Plot showing the comparison of linear models by the fit tools

3.4. Evaluation of non-linear isotherms by error function models

Like the linear forms of adsorption isotherms, different error function models are also applied to the non-linear forms of Langmuir, Freundlich, Dubinin-Radushkevich, and Temkin isotherms to find out the ideal model among all of these. The values of their error functions are summarized in Table 4. Table 5 illustrates the comparison of error function values of non-linear forms of

adsorption isotherms. It is clear from the comparison that the Dubinin-Radushkevich isotherm has the highest values of all error functions, except the HYBRID and ALCc error functions. Moreover, although the values of error functions for non-linear forms of the Freundlich isotherm are lower than Dubinin-Radushkevich, its SNE value is the highest among all other isotherms, and the R^2 value is below the R^2 values of adsorption isotherms, including Dubinin-Radushkevich, Langmuir, and Temkin. Thus, the non-linear form of the Freundlich isotherm does not fit best in the present adsorption study.

In the Langmuir isotherm, values of its error functions are lower than Freundlich isotherm; furthermore, its R^2 value is larger, and its SNE value is less than that of the Freundlich isotherm. Thus, the non-linear form of the Langmuir isotherm better fits the adsorption of Rhodamine-B compared to a non-linear form of the Freundlich isotherm.

The values of most error functions for Temkin isotherms are the least of all other isotherms. Additionally, its R^2, t-test, and F-test values are maximum, and its SNE value is lower than all non-linear forms of adsorption isotherms. As demonstrated in Figure 5. This illustrates the graphical comparison of fit tools for each non-linearized model. These outcomes suggested that the non-linear form of Temkin isotherms best describes the adsorption of Rhodamine-B dye by CaO NPs. Thus, the fitting of non-linear models follows the order Temkin > Dubinin-Radushkevich > Langmuir > Freundlich.

364 **Table 4.** Values of error functions and fit tools of non-linearized models (Fil 2023).

Error Function Model	Isotherm model (Non-Linear)			
	Langmuir	**Freundlich**	**Dubinin-Radushkevich**	**Temkin**
ERRSQ/RSS	0.306951	0.48084	1.04923E-12	0.204481724
EABS	-0.14093	-0.10288	3.80943E-07	3.07084E-06
ARE	1.5347572	1.86161	1.558145091	-0.05727
ARED/APE (%)	-6.469249693	-7.44644	6.23258	-0.22908
Chi-Sq/χ^2	0.161507	0.258304	$4.5183E^{-07}$	0.089304
G^2	-0.1282	0.034479	$1.37E^{-06}$	0.088953853
HYBRID	4.037685	6.457596006	$1.12957E^{-05}$	2.232596
ALC_c	-13.15251816	-10.9083	-28.39240104	-15.18357294
R^2	0.92024	0.875063	0.93745	**0.94687**
Students. T-Test	0.8301	0.900621	0.75282302	**0.9999954**
F-Test	0.847642	0.8476768	0.919974151	**0.9695088**
SNE	-3.19595333	-1.88597	-3.151445594	**-5.32931513**

365

366 **Table 5.** Comparison of non-linearized models by error functions (Hadi, Samarghandi et al., 2010)

Error Functions	**Isotherm Models Comparison**
ERRSQ/RSS	Dubinin-Radushkevich > Freundlich > Langmuir > Temkin
EABS	Dubinin-Radushkevich > Temkin > Freundlich > Langmuir
ARE	Dubinin-Radushkevich > Langmuir > Freundlich > Temkin
ARED/APE (%)	Dubinin-Radushkevich > Temkin > Langmuir> Freundlich
Chi-Sq/χ^2	Dubinin-Radushkevich > Freundlich > Langmuir > Temkin
G^2	Dubinin-Radushkevich > Temkin > Freundlich > Langmuir
HYBRID	Freundlich > Langmuir > Temkin > Dubinin-Radushkevich
ALC_c	Freundlich > Langmuir > Temkin > Dubinin-Radushkevich
R^2	**Temkin** > Dubinin-Radushkevich > Langmuir > Freundlich
Students' T-Test	**Temkin** > Freundlich > Langmuir > Dubinin-Radushkevich
F-Test	**Temkin** > Dubinin-Radushkevich > Freundlich > Langmuir
SNE	Freundlich > Langmuir > Dubinin-Radushkevich > **Temkin**

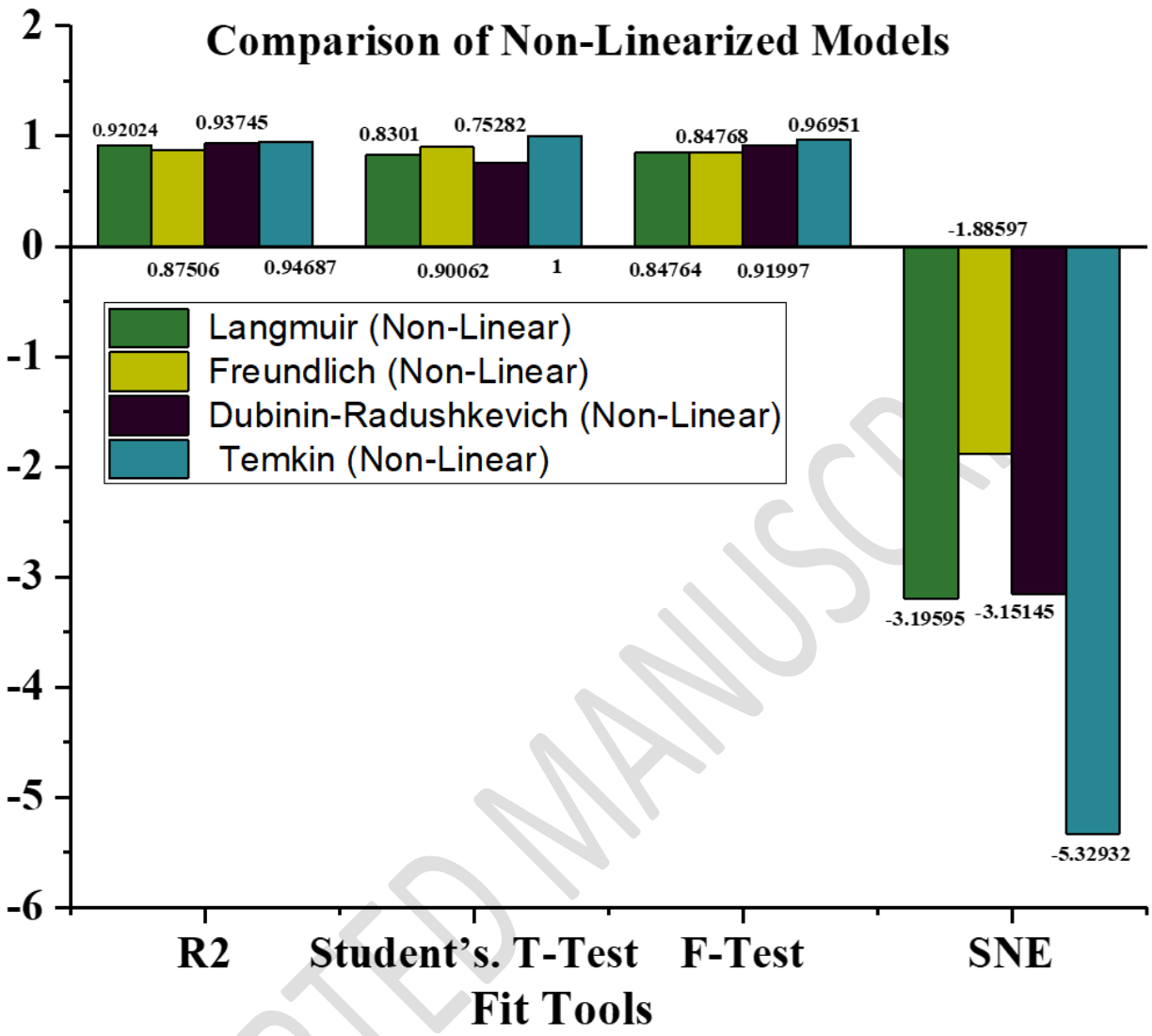

Figure 5. Comparison of non-linearized models by fit tools

3.5. The comparison of linear and non-linear forms

To identify the best model among all these isotherms, a comparison of the linear and non-linear versions of each adsorption isotherm was also carried out, utilizing a variety of error functions and fit methods. The comparison of various error functions for both forms of Langmuir isotherm indicates that values of most error functions for the non-linear form are larger than for the linear form (Table 6). A valuable comparison was performed by graphically comparing the fit tools for

both forms. Thus, a graphical comparison of fit tools for linear and non-linear forms of each adsorption isotherm is represented below. It is evident from the graphical comparison that R^2, Student's T-Test, and F-Test values of the linear form of the Langmuir isotherm are larger than the non-linear form (Figure 6). Furthermore, the sum of normalized error for the linear form is also smaller than the non-linear form, thus the linear form of the Langmuir isotherm provides a better fit than the non-linear form. The applicability of the Langmuir model to the adsorption of Rhodamine-B is reported in the literature (Khamparia and Jaspal, 2016).

Table 6. Comparison of linear and non-linear Langmuir isotherms (Rahman and Sathasivam 2015)

ERRSQ/RSS	Langmuir (Linear) < Langmuir (Non-Linear)
EABS	Langmuir (Linear) > Langmuir (Non-Linear)
ARE	Langmuir (Linear) < Langmuir (Non-Linear)
ARED/APE (%)	Langmuir (Linear) > Langmuir (Non-Linear)
Chi-Sq/χ^2	Langmuir (Linear) < Langmuir (Non-Linear)
G_2	Langmuir (Linear) > Langmuir (Non-Linear)
HYBRID	Langmuir (Linear) < Langmuir (Non-Linear)
ALCc	Langmuir (Linear) < Langmuir (Non-Linear)
R^2	**Langmuir (Linear)** > Langmuir (Non-Linear)
Students' T-test	**Langmuir (Linear)** > Langmuir (Non-Linear)
F-test	**Langmuir (Linear)** > Langmuir (Non-Linear)
SNE	**Langmuir (Linear)** < Langmuir (Non-Linear)

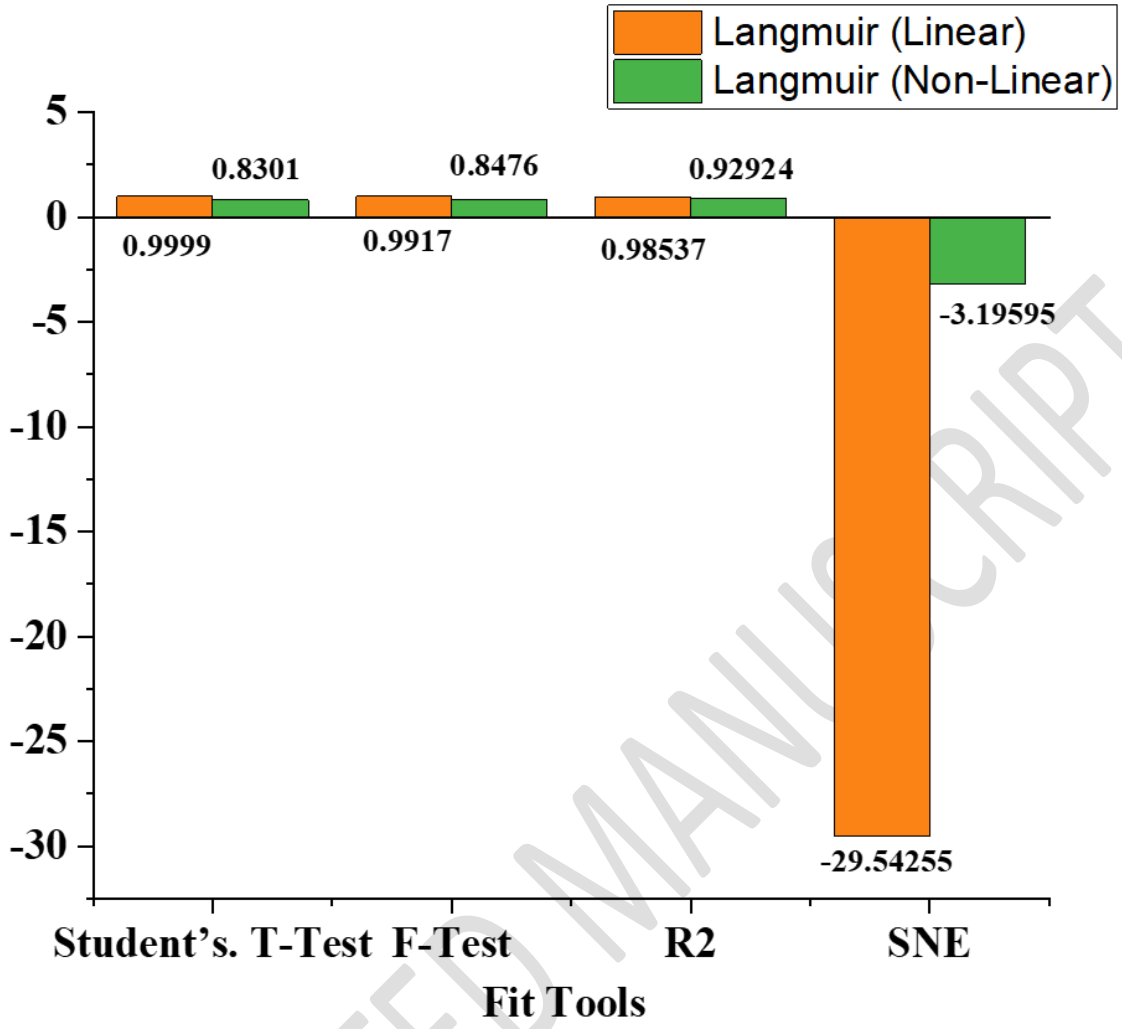

Figure 6. The relationship between linear and non-linear Langmuir isotherms with the fit tools of rhodamine-B adsorption by CaO NPs

In the same way, error function values for both linear and non-linear forms of the Freundlich isotherm were compared (Table 7). The comparison indicates that most error functions in non-linear forms have values exceeding those in linear forms. An insightful comparison was obtained by comparing the fit tools provided in Figure 7. R^2, T-test, and F-test values are larger for the linear form, but the standard procedure (sum of normalized error) value is smaller for the non-linear form. As a result, the non-linear form of the Freundlich isotherm is more compatible than the linear form.

397 **Table 7.** Comparison of linear and non-linear Freundlich models

ERRSQ/RSS	Freundlich (Linear) < Freundlich (Non-Linear)
EABS	Freundlich (Linear) < Freundlich (Non-Linear)
ARE	Freundlich (Linear) > Freundlich (Non-Linear)
ARED/APE (%)	Freundlich (Linear) > Freundlich (Non-Linear)
Chi-Sq/χ^2	Freundlich (Linear) < Freundlich (Non-Linear)
G^2	Freundlich (Linear) < Freundlich (Non-Linear)
HYBRID	Freundlich (Linear) < Freundlich (Non-Linear)
ALC_c	Freundlich (Linear) > Freundlich (Non-Linear)
R^2	Freundlich (Linear) > Freundlich (Non-Linear)
Students' T-test	Freundlich (Linear) > Freundlich (Non-Linear)
F-test	Freundlich (Linear) > Freundlich (Non-Linear)
SNE	Freundlich (Linear) > **Freundlich (Non-Linear)**

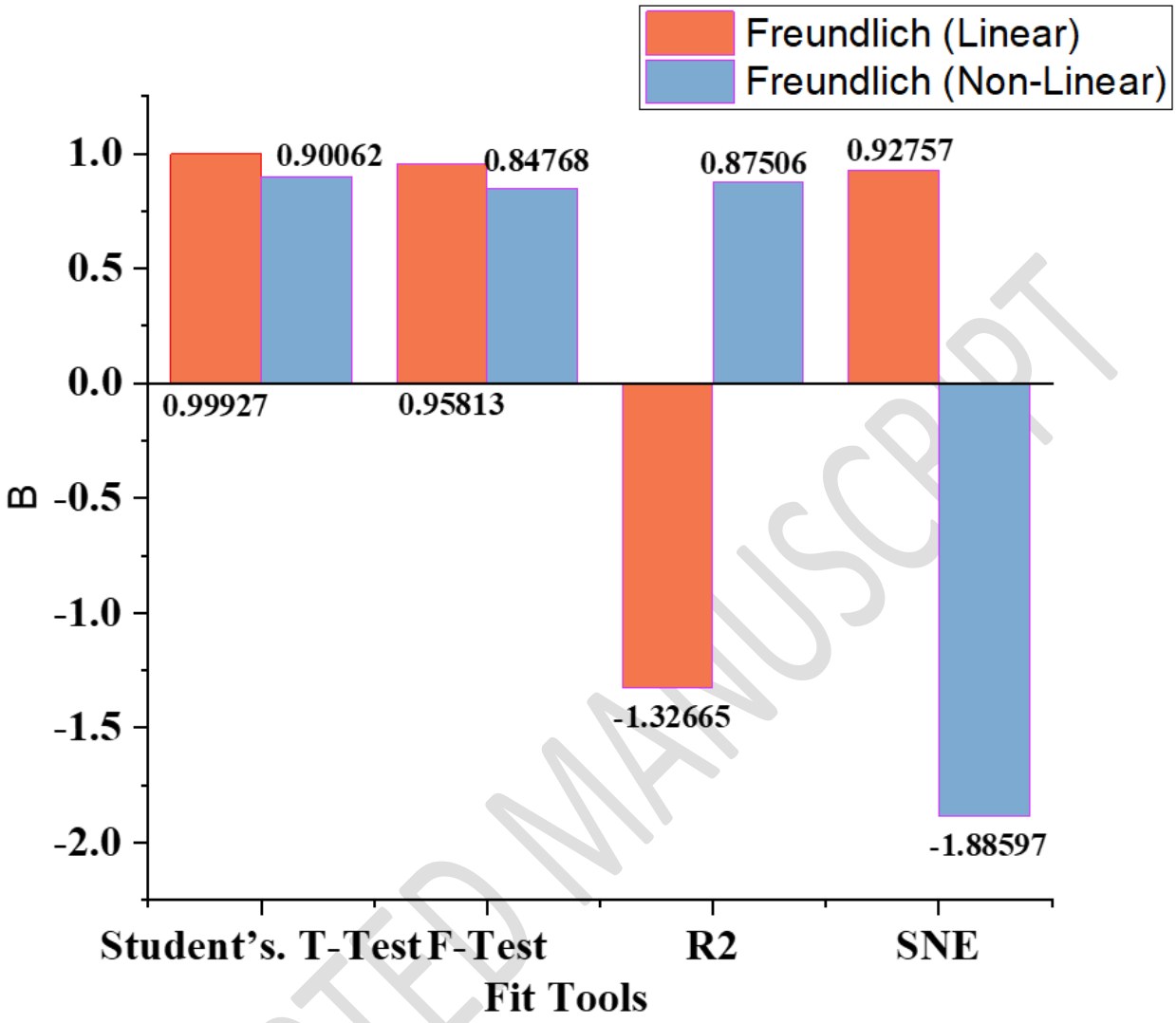

Figure 7. The relationship between linear and non-linear Freundlich isotherms with fit tools

The analysis of linear and non-linear forms of the Dubinin-Radushkevich isotherm illustrated that non-linear forms have the highest values of the error function, and lower values of fit tools such as R^2, T-test, and F-test (Figure 8 and Table 8). Furthermore, the value of SNE was also found to be larger than that of the linear form. The outcome of this evaluation of both forms suggested more applicability of the linear form than the non-linear form of this model.

407 **Table 8.** Comparison of linear and non-linear Dubinin Radushkevich models

ERRSQ/RSS	Dubinin-Radushkevich (Linear) < Dubinin-Radushkevich (Non-Linear)
EABS	Dubinin-Radushkevich (Linear) < Dubinin-Radushkevich (Non-Linear)
ARE	Dubinin-Radushkevich (Linear) < Dubinin-Radushkevich (Non-Linear)
ARED/APE (%)	Dubinin-Radushkevich (Linear) < Dubinin-Radushkevich (Non-Linear)
Chi-Sq/χ^2	Dubinin-Radushkevich (Linear) < Dubinin-Radushkevich (Non-Linear)
G^2	Dubinin-Radushkevich (Linear) < Dubinin-Radushkevich (Non-Linear)
HYBRID	Dubinin-Radushkevich (Linear) < Dubinin-Radushkevich (Non-Linear)
ALCc	Dubinin-Radushkevich (Linear) > Dubinin-Radushkevich (Non-Linear)
R^2	Dubinin-Radushkevich (Linear) > Dubinin-Radushkevich (Non-Linear)
Student's T-test	Dubinin-Radushkevich (Linear) > Dubinin-Radushkevich (Non-Linear)
F-test	Dubinin-Radushkevich (Linear) > Dubinin-Radushkevich (Non-Linear)
SNE	Dubinin-Radushkevich (Linear) < **Dubinin-Radushkevich (Non-Linear)**

408

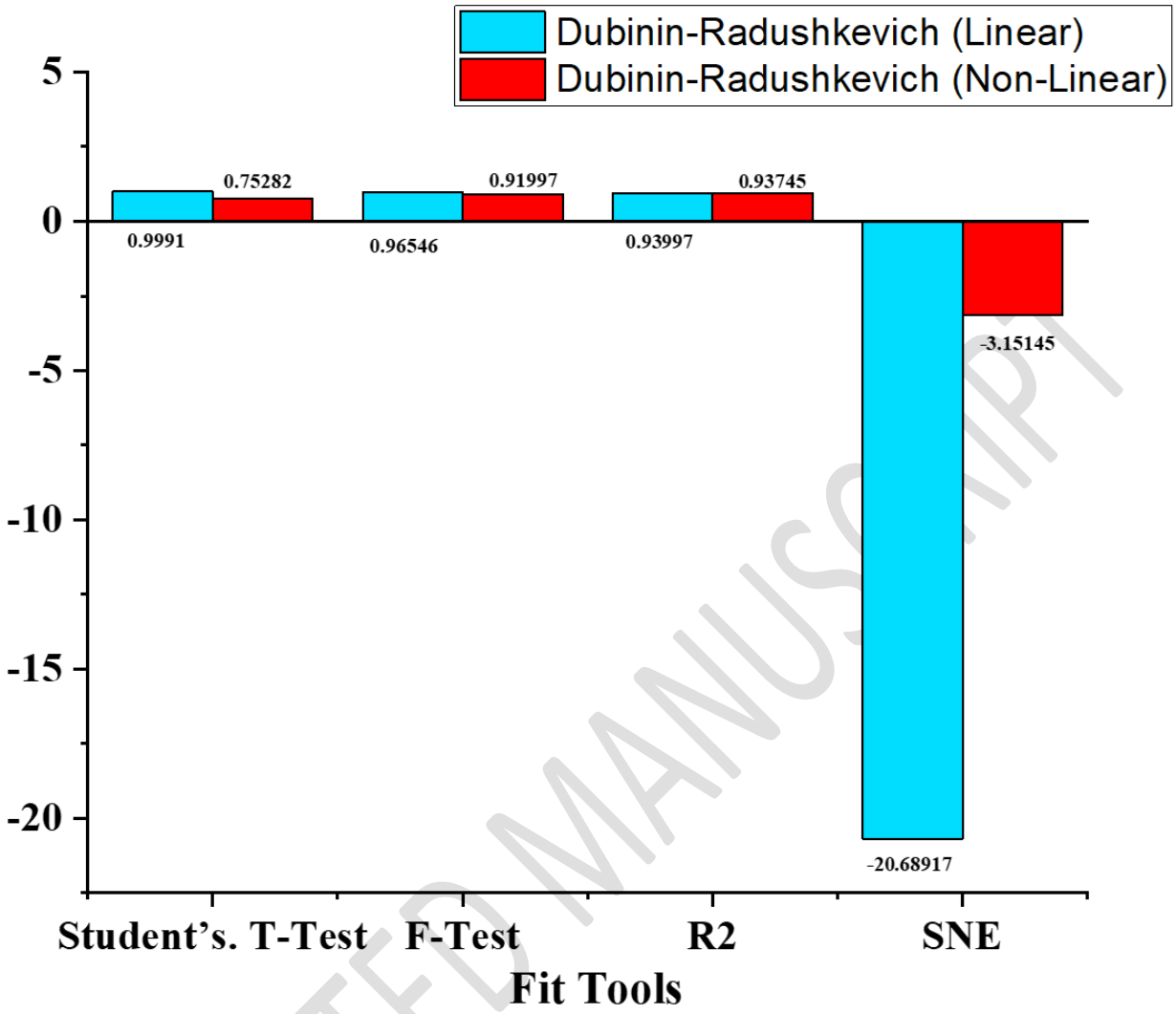

409

410 **Figure 8.** The relationship between linear and non-linear Dubinin-Radushkevich isotherms with

411 fit tools

412

413 While analyzing the error function and fit tool values for linear and non-linear forms of the Temkin

414 model, it was revealed that no issues were encountered while transforming the non-linear Temkin

415 form into its linear form (Table 9 and Figure 9). Moreover, the values of error functions were found

416 same for both forms. Both forms of the Temkin isotherm were proven better for the present

417 adsorption study.

418

419 **Table 9.** Comparison of linear and non-linear Temkin models (Sivarajasekar and Baskar 2014)

ERRSQ/RSS	Temkin (Linear) = Temkin (Non-Linear)
EABS	Temkin (Linear) < Temkin (Non-Linear)
ARE	Temkin (Linear) = Temkin (Non-Linear)
ARED/APE (%)	Temkin (Linear) = Temkin (Non-Linear)
Chi-Sq/χ^2	Temkin (Linear) = Temkin (Non-Linear)
G2	Temkin (Linear) = Temkin (Non-Linear)
HYBRID	Temkin (Linear) = Temkin (Non-Linear)
ALCc	Temkin (Linear) = Temkin (Non-Linear)
R2	Temkin (Linear) = Temkin (Non-Linear)
Students' T-Test	Temkin (Linear) = Temkin (Non-Linear)
F-Test	Temkin (Linear) = Temkin (Non-Linear)
SNE	**Temkin (Linear) = Temkin (Non-Linear)**

420

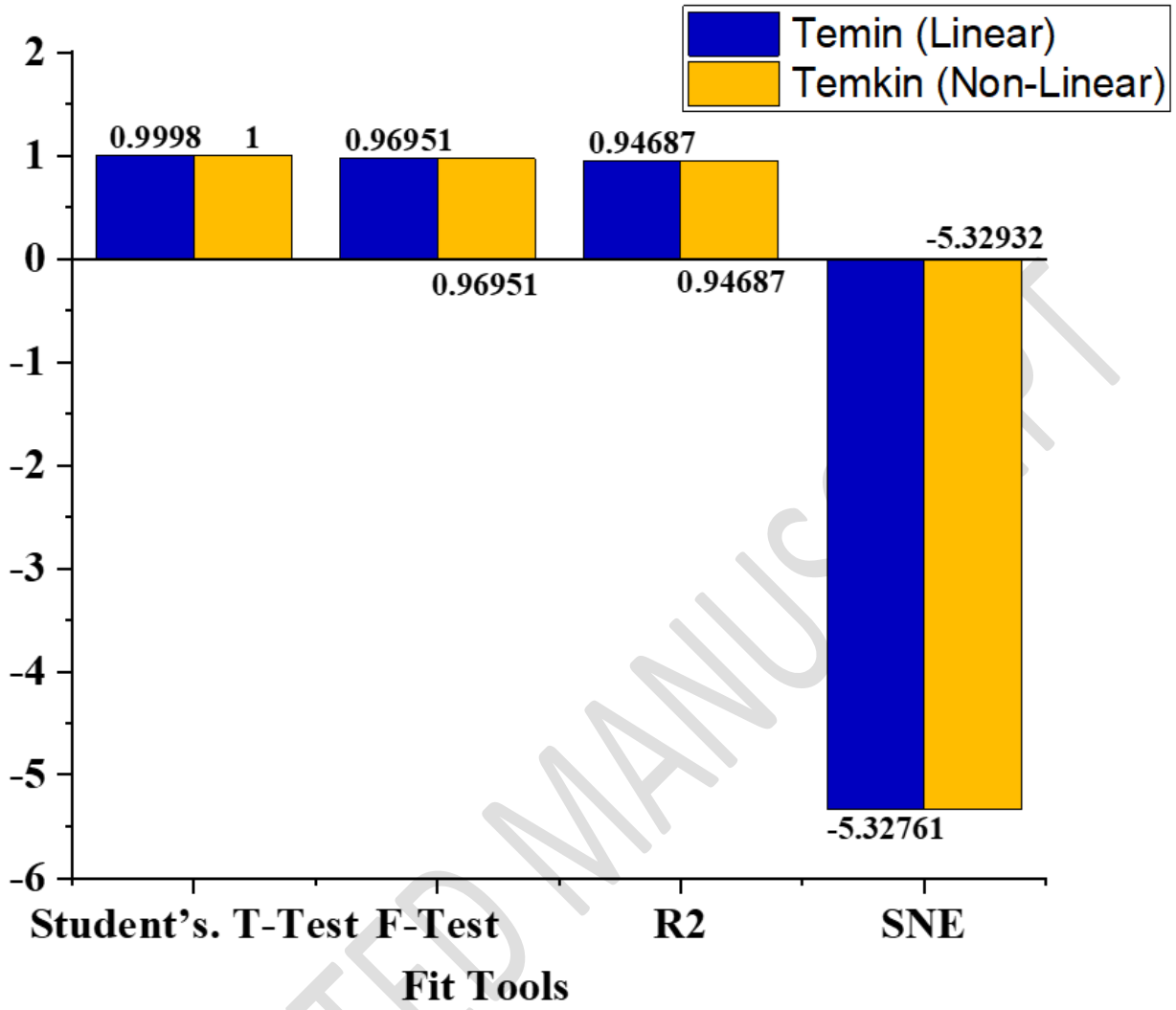

Figure 9. The relationship between linear and non-linear Temkin isotherms with fit tools

4. CONCLUSIONS

The linear and non-linear forms of each adsorption isotherm were contrasted. Error functions such as ERRSQ/RSS, ARE, EABS, APE/ARED, (ALC_c), (Chi-Sq/χ^2), G^2, HYBRID, a standard procedure called the sum of normalized errors (SNE), and fit tools including (R^2), Student's T-test, and F-tests were successfully applied to each form. This study proceeded by contrasting all linear forms with each other, evaluating all non-linear forms with each other, and finally comparing each

non-linear form with non-linear forms of adsorption isotherms to analyze the most applicable model to the adsorption of Rhodamine-B by CaO NPs. The results indicated that the Langmuir isotherm was identified as more suitable (T-test = 0.999981, F-test = 0.991724664, and R^2 = 0.98537) than all other linear forms. Likewise, the analysis of non-linear forms provided the Temkin model as more beneficial, with the lowest values of all error functions and the largest values of fit tools, including R_2 (0.94687), T-test (0.969513), and F-test (0.999998). Evaluation of each linear form with a non-linear form illustrated the following results. The linear Langmuir model was noted as best fitted with the largest values of fit tools and lowest normalized errors (0.0077098) than the non-linear Langmuir isotherm (0.306951). Non-linear Freundlich was identified as more beneficial than the linear Freundlich isotherm. The linear Dubinin-Radushkevich isotherm best describes the present adsorption study better than the non-linear Dubinin-Radushkevich model. In the Temkin isotherm, the conversion of the non-linear form into its linear form proceeded without any problem. Moreover, they had the same error functions and isothermal parameters. As a result, it was shown that non-linear modeling significantly better represents experimental data than linearized models, with the total meaning of the error functions in linearized models being noticeably larger than in the non-linear model. The ideal parameters for the isothermal equation in this system are given by the error function. The isotherm parameters need to be regarded as more accurate for use in the design of commercial adsorbers because they differ from the values derived from linearized data analysis.

The kinetic data would help create suitable wastewater treatment design technology. The pseudo-second-order chemical reaction kinetics offer the best correlation of the experimental data, and chemical reactions appear to be important in the rate-controlling step for all systems under study. The present work successfully describes the linear and nonlinear forms of the models and error

functions. However, there is a limitation of the present work that a limited dataset is utilized for the modeling purpose as well as error analysis. For future work, it is recommended to apply these models on a large data set, also the use of the predicted dataset adds more knowledge for the readers. A comprehensive study of the methods to overcome these errors is also required to be addressed.

Author contribution statement

G.N.: Writing – original draft, Writing – review & editing, Visualization, Validation, Software, Resources, Methodology, Formal analysis. **F.B.**: Writing – original draft, Writing – review & editing, Visualization, Validation, Supervision, Software, Resources, Project administration, Methodology, Funding acquisition, Formal analysis. **T.I., N.S., S.L., M.S., E.S., M.T., and M.M.**: Writing – review & major editing, Visualization, Validation, Software, Resources, Methodology, Investigation, Formal analysis, Data curation, Conceptualization. **A.D., G.D.A-Q., and M.A.M.:** Writing – review & major editing, Visualization, Investigation, Validation, Software, Resources, Project administration, Methodology, Formal analysis, Conceptualization. All authors read and approved of the final manuscript.

Declaration of competing interests

The authors declare that they have no known competing financial interests or personal relationships that could have appeared to influence the work reported in this paper.

Data availability

Data will be made available on request from the corresponding author.

Acknowledgments

The authors extend their appreciation to the Ongoing Research Funding program - Research Chairs (ORF-RC-2025-5512), King Saud University, Riyadh, Saudi Arabia. We are thankful to the University of Sargodha for the Provision of research facilities.

Funding

Ongoing Research Funding program - Research Chairs (ORF-RC-2025-5512), King Saud University, Riyadh, Saudi Arabia.

References

Abdulhameed A.S., Al Omari R.H., Alsayer I.A., Abualhaija M., and Algburi S. (2025). Optimized adsorption of methylene blue dye onto bio-based citric acid-modified oleander (Nerium oleander) leaves/chitosan adsorbent using Box-Behnken design approach. *Biomass Conversion and Biorefinery*, 1-23.

Akhtar M.S., Jutt D.S.R., Aslam S., Nawaz R., Irshad M.A., Khan M., Khairy M., Irfan A., Al-Hussain S.A., and Zaki M.E. (2024). Green synthesis of graphene oxide and magnetite nanoparticles and their arsenic removal efficiency from arsenic-contaminated soil. *Scientific Reports*, **14**(1), 23094.

Aslam A., Batool F., Noreen S., Abdelrahman E.A., Mustaqeem M., Albalawi B.F.A., Ditta A. (2024). Metal oxide impregnated biochar for azo dyes remediation as revealed through kinetics, thermodynamics, and response surface methodology. *ACS Omega*, **9** (4), 4300-4316

Batool F., Tahira M., Gul M., Qadir R., Akhtar T., Ghumman S.A., Amin M., Sajjad N., Rehman M.A., Ditta A. (2025). Bioremediation of Nigrosine Anionic Dye from Wastewater Employing Copper Nanocomposite-Modified Cucumis melo Seeds Powder: A Comparison of Performance

Evaluation between Defatted and Surface Modified Adsorbent. *Biomass Conversion and Biorefinery*, 1-20.

Benmessaoud A., Nibou D., Mekatel E.H., and Amokrane S. (2020). A comparative study of the linear and non-linear methods for the determination of the optimum equilibrium isotherm for the adsorption of Pb^{2+} ions onto Algerian treated clay. *Iranian Journal of Chemistry and Chemical Engineering (IJCCE)*, **39**(4), 153-171.

Chauhan S., Mohanty A., and Meena S.S. (2025). Unlocking the potential of rhamnolipids: production via agro-industrial waste valorization, market insights, recent advances, and applications. *Biomass Conversion and Biorefinery*, 1-30.

Chen X., Li M., He J., Wu Y., Sun J., and Wen X. (2025). Waste cotton-based activated carbon with excellent adsorption performance towards dyes and antibiotics. *Chemosphere*, **376**, 144292.

Dixit U., Singh K., Mohan S., Singh A.K., and Kumar A. (2024). Surface activity, mechanisms, kinetics, and thermodynamic study of adsorption of malachite green dye onto sulfuric acid-functionalized Moringa oleifera leaves from aqueous solution. *Environmental Monitoring and Assessment*, **196**(1), 78.

Dubinin M. (1960). The potential theory of adsorption of gases and vapors for adsorbents with energetically nonuniform surfaces. *Chemical Reviews*, **60**(2): 235-241.

Fil B.A. (2023). Investigation of the adsorption of basic orange 2 dye on montmorillonite and error analysis. *Bulletin of the Chemical Society of Ethiopia*, **37**(1), 47-58.

Foo K.Y. and Hameed B.H. (2010). Insights into the modeling of adsorption isotherm systems. *Chemical Engineering Journal*, **156**(1), 2-10.

Freundlich H.M.F. (1906). Over the adsorption in solution. *Journal of Physical Chemistry*, **57**(385471), 1100-1107.

Hadi M., Samarghandi M. R., and McKay G. (2010). Equilibrium two-parameter isotherms of acid dyes sorption by activated carbons: study of residual errors. *Chemical Engineering Journal*, **160**(2), 408-416.

Hadi M., Samarghandi M.R., and McKay G. (2010). Equilibrium two-parameter isotherms of acid dyes sorption by activated carbons: study of residual errors. *Chemical Engineering Journal*, **160**(2), 408-416.

Hanafiah Z.M., Mohtar W.H.M.W., Rohani R., Fadzizi M.F., Wan W.A.A.Q.I., Sayed K., Manan T.S.B.A., and Indarto A. (2024). Removal of pharmaceutical compounds from sewage effluent by the nanofiltration membrane. *Journal of Water Process Engineering*, **68**, 106320.

Ifelebuegu A.O. (2012). Removal of steroid hormones by activated carbon adsorption—kinetic and thermodynamic studies. *Journal of Environmental Protection*, **3**(6), 469-475.

Inyinbor A., Adekola F., and Olatunji G.A. (2016). Kinetics, isotherms, and thermodynamic modeling of liquid phase adsorption of Rhodamine B dye onto Raphia hookerie fruit epicarp. *Water Resources and Industry*, **15**, 14-27.

Kanwal S., Batool F., Sharif G., Naeem H.K., Noreen S., Gondal H.Y., Kamal U.B., Ditta A. (2024). Guar gum, *Ulva lactuca* L. biomass, and xanthan gum-based copolymer novel biosorbent for adsorptive removal of acid orange 10. *Biocatalysis and Agricultural Biotechnology*, **58**, 103173

Kapoor A., and Yang R. (1989). Correlation of equilibrium adsorption data of condensible vapors on porous adsorbents. *Gas Separation & Purification*, **3**(4), 187-192.

Khamparia S., and Jaspal D. (2016). Investigation of the adsorption of Rhodamine B onto a natural adsorbent, *Argemone mexicana*. *Journal of Environmental Management*, **183**, 786-793.

Kumar K.V., and Porkodi K. (2006). Relation between some two- and three-parameter isotherm models for the sorption of methylene blue onto lemon peel. *Journal of Hazardous Materials*, **138**(3), 633-635.

Kumar K.V., and Sivanesan S. (2006). Pseudo-second order kinetics and pseudo isotherms for malachite green onto activated carbon: comparison of linear and non-linear regression methods. *Journal of Hazardous Materials*, **136**(3), 721-726.

Latif S., Zahid A., Batool F., Kanwal S., Ditta A. (2025). Adsorptive removal of Congo red dye from industrial effluent using cotton calyx iron oxide (CC-Fe_3O_4) composite. *Environmental Monitoring and Assessment*, **197**, 249.

Lavecchia R., Zuorro A., Baaloudj O., and Brienza M. (2024). Trimethoprim removal from aqueous solutions via volcanic ash-soil adsorption: process modeling and optimization. *Water*, **16**(15), 2209.

Liu C., Crini G., Wilson L.D., Balasubramanian P., and Li F. (2024). Removal of contaminants present in water and wastewater by cyclodextrin-based adsorbents: A bibliometric review from 1993 to 2022. *Environmental Pollution*, **348**, 123815.

Mahajan T., Paikaray S., and Mahajan P. (2023). Applicability of the equilibrium adsorption isotherms and the statistical tools on them: a case study for the adsorption of fluoride onto Mg-Fe-CO3 LDH. *Journal of Physics: Conference Series*. IOP Publishing.

Mahesh Y., Panwar J., and Gupta S. (2024). Remediation of multifarious metal ions and molecular docking assessment for pathogenic microbe disinfection in aqueous solution by waste-derived Ca-MOF. *Environmental Science and Pollution Research*, **31**(14), 21545-21567.

Mohamed E.A., Ahmed H.M., Altalhi A.A., Al-Shamiri H.A., and Negm N.A. (2025). Highly efficient and rapid removal of Congo red dye from textile wastewater using facilely synthesized Mg/Ni/Al layered double hydroxide. *Scientific Reports*, **15**(1), 2183.

Nasir G, Batool F, Iqbal S, Akbar J, Noreen S, Munawar KS, Iqbal T, Ditta A. (2025). Biosynthesis of lead oxide nanoparticles using mulberry leaf extract for the adsorptive removal of diazine black dye. *Biomass Conversion and Biorefinery*, **15**, 12525–12549

Nebaghe K., El Boundati Y., Ziat K., Naji A., Rghioui L., and Saidi M. (2016). Comparison of linear and non-linear methods for the determination of optimum equilibrium isotherm for the adsorption of copper (II) onto treated Martil sand. *Fluid Phase Equilibria*, **430**, 188-194.

Nisar B., Yasin M., Batool F., Mahmood H., Rubab S.L., Sultan A., Mustaqeem M., Ditta A., Iqbal R., Gurbanova L., Al-Khayri J.M. (2025). A green approach for the treatment of industrial effluent for hazardous metals of chromium and lead. *Global NEST Journal*, **27**(10), 07611.

Outram J.G., Couperthwaite S.J., Martens W., and Millar G.J. (2021). Application of non-linear regression analysis and statistical testing to equilibrium isotherms: Building an Excel template and interpretation. *Separation and Purification Technology*, **258**, 118005.

Paluri P., Ahmad K.A., and Durbha K.S. (2022). Importance of estimation of optimum isotherm model parameters for adsorption of methylene blue onto biomass-derived activated carbons: Comparison between linear and non-linear methods. *Biomass Conversion and Biorefinery*, **12**(9), 4031-4048.

Radha E., Gomathi T., Sudha P.N., Latha S., Ghfar A.A., and Hossain N. (2025). Adsorption studies on the removal of Pb (II) and Cd (II) ions using chitosan-derived copolymeric blend. *Biomass Conversion and Biorefinery*, **15**(2), 1847-1862.

585 Rahman M.S. and Sathasivam K.V. (2015). Heavy metal adsorption onto Kappaphycus sp. from
586 aqueous solutions: the use of error functions for validation of isotherm and kinetics models.
587 *BioMed Research International*, **2015**(1), 126298.
588 Rana R., and Singhal R. (2015). Chi-square test and its application in hypothesis testing. *Journal*
589 *of Primary Care Specialties*, **1**(1), 69-71.
590 Sayed K., Hanna W., Hanafiah Z.M., Bithi A.S. and Abd W. (2024b). Removal of pharmaceuticals
591 from municipal wastewater using Malaysian Ganoderma Lucidum Fungal Strain. *Jurnal*
592 *Kejuruteraan*, **36**(4), 1467-1476.
593 Sayed K., Mohtar W.H.M.W., Hanafiah Z.M., Wan W.A.A.Q.I., Abd Manan T.S.B. and Sharif
594 S.A.B.M. (2024a). Simultaneous enhanced removal of pharmaceuticals and hormones from
595 wastewaters using series combinations of ultra-violet irradiation, bioremediation, and adsorption
596 technologies. *Journal of Water Process Engineering*, **57**, 104589.
597 Selvanarayanan R., Rajendran S., Pappa C. K., and Thomas B. (2024), Wastewater recycling to
598 enhance environmental quality using fuzzy embedded with RNN-IOT for sustainable coffee
599 farming, *Global NEST Journal*, **26**(8), 06346. https://doi.org/10.30955/gnj.06346.
600 Sivarajasekar N. and Baskar R. (2014). Adsorption of basic red 9 onto activated carbon derived
601 from immature cotton seeds: isotherm studies and error analysis. *Desalination and Water*
602 *Treatment*, **52**(40-42), 7743-7765.
603 Slimani R., El Ouahabi I., Abidi F., El Haddad M., Regti A., Laamari M.R., El Antri S. and Lazar
604 S. (2014). Calcined eggshells as a new biosorbent to remove basic dye from aqueous solutions:
605 thermodynamics, kinetics, isotherms, and error analysis. *Journal of the Taiwan Institute of*
606 *Chemical Engineers*, **45**(4), 1578-1587.

Suresh M., Surendran R., Raveena S., and Gowri S. (2025), Wastewater Recycling Integration with IoT Sensor Vision for Real-time Monitoring and Transforming Polluted Ponds into Clean Ponds using HG-RNN, *Global NEST Journal*, https://doi.org/10.30955/gnj.06758

Temkin M. (1940). Kinetics of ammonia synthesis on promoted iron catalysts. *Acta Physiochim. URSS*, **12**, 327-356.

Umeh C.T., Nduka J.K., Mogale R., Akpomie K.G. and Okoye N.H. (2024). Acid-activated corn silk as a promising phytosorbent for uptake of Malachite green and Cd (II) ion from simulated wastewater: equilibrium, kinetic, and thermodynamic studies. *International Journal of Phytoremediation*, **26**(10), 1593-1610.

Usman M., Batool F., Iqbal T., Noreen S., Gondal H.Y., Roheen T., Qadir R., Amin M., Sajid S., Ditta A. (2025). Harnessing de-oiled *Glycine max* seeds-anchored-CuO nanoparticles for adsorptive removal of crystal violet dye with comprehensive mechanistic insights. *RSC Advances*, **15**, 24406-24423.

Venkatraman M., Surendran R., Srinivasulu S., and Vijayakumar K. (2024), Water quality prediction and classification using attention-based deep differential recurflownet with logistic giant armadillo optimization, *Global NEST Journal*, **27**(1), 06799. https://doi.org/10.30955/gnj.0679.

Voudrias E., Fytianos K., and Bozani E. (2002). Sorption–desorption isotherms of dyes from aqueous solutions and wastewaters with different sorbent materials. *Global Nest Journal*, **4**(1), 75-83.